Bayesian Reconstruction of Goal Orientated Error Fields in Large Aerospace Finite Element Models

Matthew S. Bonney[1], **Richard Evans**[1], **James Rouse**[1], **Arthur Jones**[1], and **Maxime Hamadi**[2]

[1] *The University of Nottingham, Nottingham UK, email: James.Rouse@nottingham.ac.uk*
[2] *Airbus, Toulouse France*

Keywords

GOEE, Aerospace Structures, Bayesian Response Surface, MARQUESS, Zienkiwicz-Zhu Recovery, Finite Element Method

Abstract

A major difficulty in the mechanical simulation of large aerospace structures is the multi-scale nature of modern designs due to, at least in part, the increased use of composite materials. "Thin" materials are typically idealised by shell elements in order to make simulations computationally tractable, however this significantly limits the fidelity of solutions. Through thickness stress states, for example, are important in predicting delamination but are known to be poorly approximated by shell element. To solve this issue, a multi-scale methodology, such as MARQUESS, is required to accurately model these systems. This work is focused on the application of a goal oriented error estimator methodology in MARQUESS to suggest confidence bounds of "hot-spot" predictions. The goal oriented error estimator uses the combination of dual formulations and Zienkiwicz-Zhu recovery to estimate volume averaged errors at training locations in a candidate structure. Bayesian recovery processes are then used to approximate full error fields from local solutions. This estimator is applied to two systems, one 2D system and one full 3D system, both modelled using shell elements. The 2D system investigates the mesh refinement to denote the convergence properties of the estimator. For the 3D system, the Gaussian process is used to reduce the number of dual problems from $1,300$ to 100 simulations with only small differences from the full simulations. This work demonstrates the initial implementation of this non-intrusive estimator to denote the error associated with the modelling in the macro-level scale.

1 Introduction

One difficulty in the modelling of large aerospace structures is the multi-scale nature of the modern designs with the inclusion of light-weight composite materials. Refined modelling of the large assemblies in detail is impractical while modelling only at the macro scale loses the information about the composite nature of the construction. For example, individual lamina and associated inter-lamina behaviours are not typically represented in large models, where the preferred modelling uses a simplified two dimensional representation (or "shells"). One method to accurately recover these details for this type of system is to utilize a multi-scale approach such as the methodology used in MARQUESS, which uses a bottom-up and top-down approach [1, 2]. In MARQUESS, pre-computed solutions of detailed "feature" models are used in conjuncture with the simplified global model to approximate material responses in regions of interest. This work is the preliminary evaluations of the error estimator aspect of MARQUESS.

To achieve confidence in the simulations results, errors from both the bottom-up and top-down modelling procedures must be considered. In particular, error estimation techniques must be non-intrusive as it is often the case where only "orphan" meshes (only node locations and element connectivity with no physical model) are available. This paper focuses on the top-down procedure to demonstrate the implementation on simplified systems. A similar approach can also be done on the bottom-up procedure and combined to give a global error estimate. While not presented in this work, it is part of continuing research for MARQUESS.

The error estimation technique used in this work is a goal oriented error estimator (GOEE) [3, 4, 5] that utilizes the Zienkiwicz-Zhu (ZZ) [6, 7, 8] recovery based error estimator for selected goal Quantities of Interest (QoIs) such as average stress in a region. These QoIs can be computed through a dual (or adjunct) problem

that performs a secondary simulation [5]. Using a dual problem helps alleviate some of the intrusive requirements that are often required for particular QoIs. This error estimator method can identify "hot-spots" that might require more attention from the design engineer for further specification, mesh refinement, or a region to pay attention to if there is any design modifications on other parts/sections of the system. One of the major issues with this method is the large number of computational evaluations required to solve these QoIs. This work reduces this computational burden through the use of Bayesian surface identification/sampling via Gaussian Process (GP) by using training simulations then sampling instead of performing a full simulation for each QoI.

This paper looks at two systems and applies the general work-flow to both of these systems. The first system is a simplified 2D flat panel to help demonstrate the work-flow and to ensure the accuracy of the implementation. For this system, only one QoI is used, thus the Bayesian surface identification is not performed. The second system is a portion of a stiffened panel subjected to a bending load. This is used to demonstrate the GP for multiple QoIs and to show a more realistic system in 3D. This paper is organized as follows: the general work-flow along with the underlying theories are presented in Section 2. Within this section, several subsections explain the theory to the many individual parts of the work-flow. Section 3 goes through the 2D flat panel system and the results, while Section 4 discusses the 3D stiffened panel and the analysis performed on it. This paper is concluded with some remarks and expected future work in Section 5.

2 Methodology and Theory

The general methodology of this work follows the flowchart in Fig. 1. In this work-flow, there are five main aspects that will be discussed in this section. The first is the Finite Element (FE) formulation used in this work. In an ideal case, this work would use ABAQUS for these simulations. Unfortunately, ABAQUS acts as a black-box and prevents (or greatly hides) some of the information needed for this work. In particular, the deformation matrix and stress/strains at each integration location. While these are required calculations, they are not easily accessible outside of the black-box. To alleviate this issue, a similar element is custom programmed in MatLab with future work to incorporate this into ABAQUS for industrial use with the use of an user-defined element. This custom element is discussed in Section 2.1.

The second section for discussion is the aspect of the primal and dual system. In general, the primal system is the ordinary force-stiffness-displacement calculation while the dual system uses the same stiffness, but solves a different linear system, which is discussed in Section 2.2. The ZZ recovery method is discussed in Section 2.3 and is used in the GOEE, discussed in Section 2.4. Finally, a discussion of the Bayesian response surface/GP is discussed in Section 2.5. One aspect to note is that the Bayesian response surface is only applied to the 3D stiffened panel in Section 4.

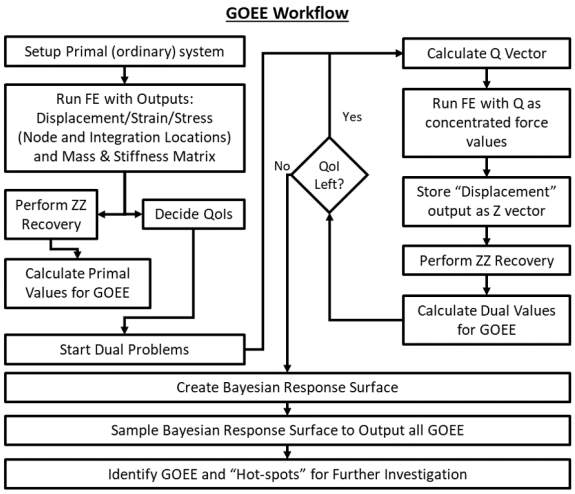

Figure 1: General methodology

2.1 Finite Element Model Formulation

Commercial finite element codes, such as ABAQUS [9], are widely used for the structural analysis of components and structures within industrial applications. However, for the purposes of this work, additional information is required to calculate the error estimator which not returned by ABAQUS to the user. To overcome this, a custom shell element has been developed for the simulation of 3D components [10, 11]. This work uses a general-purpose, iso-parametric, degenerate continuum shell element formulation, where small strains with linear material and geometric properties are assumed.

The shell element uses a bi-linear interpolation with 4 nodes, with 2x2 Gauss points for the bending and membrane and a single point contribution for shear [12]. With the rotational degree of freedom (DOF) about the z-axis, often termed the drilling DOF, neglected due to the thin nature of the elements. For the purpose of this paper, as the mid-surface is assumed as flat (not curved) the shell element can essentially be classified by the super-position of plane stress and plate bending, where the effects of bending and membrane actions are assessed independently [13]. The internal energy is defined for each element by a linear geometric interpolation scheme throughout the element, ex-

pressed as

$$U^e = \frac{1}{2}\int_{\Omega_e} \sigma_b \cdot \epsilon_b d\Omega_e + \frac{1}{2}\int_{\Omega_e} \sigma_m \cdot \epsilon_m \Omega_e + \frac{\kappa}{2}\int_{\Omega_e} \sigma_s \cdot \epsilon_s \Omega_e, \tag{1}$$

where σ_α and ϵ_α are defined for the corresponding bending, membrane and shear components $\{\alpha\}$ for each element domain Ω_e, and $\sigma_\alpha \cdot \epsilon_\alpha$ is the tensor dot product of the stress and strain. The linear-elastic stress-strain relations are defined for a homogeneous isotropic material as

$$\sigma_\alpha = C_\alpha \cdot \epsilon_\alpha, \tag{2}$$

where ϵ_α is the applied strain and the material material matrix C_α is defined by the constitutive equation for plane stress as

$$C_m = \frac{Et}{(1-v^2)}\begin{bmatrix} 1 & \nu & 0 \\ \nu & 1 & 0 \\ 0 & 0 & \left(\frac{1-\nu}{2}\right) \end{bmatrix} \tag{3a}$$

$$C_b = \left(\frac{t^2}{12}\right) C_m \tag{3b}$$

$$C_s = \begin{bmatrix} G & 0 \\ 0 & G \end{bmatrix}, \tag{3c}$$

where E and ν are the material Young's modulus and Poisson's ration, t is the thickness, which is constant over the shell, and G is the shear modulus given as

$$G = \kappa \frac{Et}{2\,(1+\nu)}, \tag{4}$$

where κ is an additional correction factor, taken as 5/6.

The generalised strain-displacements for bending, membrane and shear are independently interpolated in the local coordinates by

$$u\,(x,y) = \begin{bmatrix} u_x \\ u_y \\ u_z \\ \theta_x \\ \theta_y \\ \theta_z \end{bmatrix} = \sum_{i=1}^{4} u_i N_i\,(\xi,\eta)\,, \tag{5}$$

where $N_i(\xi,\eta)$ are the shape functions of a standard bi-linear four node element. With bending, membrane and shear strains computed from displacements via:

$$\epsilon_\alpha = B_\alpha d^e. \tag{6}$$

The strain-displacement matrices (B_α) are defined by the derivation of the shape functions by defining individual matrices as given in Eq. 7.

$$B_b^{(e)} = \begin{bmatrix} 0 & 0 & 0 & 0 & \frac{\partial N_1}{\partial x} & 0 & \dots & 0 & 0 & 0 & 0 & \frac{\partial N_4}{\partial x} & 0 \\ 0 & 0 & 0 & \frac{\partial N_1}{\partial y} & 0 & 0 & \dots & 0 & 0 & 0 & \frac{\partial N_4}{\partial y} & 0 & 0 \\ 0 & 0 & 0 & \frac{\partial N_1}{\partial x} & \frac{\partial N_1}{\partial y} & 0 & \dots & 0 & 0 & 0 & \frac{\partial N_4}{\partial x} & \frac{\partial N_4}{\partial y} & 0 \end{bmatrix} \tag{7a}$$

$$B_m^{(e)} = \begin{bmatrix} \frac{\partial N_1}{\partial x} & 0 & 0 & 0 & 0 & 0 & \dots & \frac{\partial N_4}{\partial x} & 0 & 0 & 0 & 0 & 0 \\ 0 & \frac{\partial N_1}{\partial y} & 0 & 0 & 0 & 0 & \dots & 0 & \frac{\partial N_4}{\partial y} & 0 & 0 & 0 & 0 \\ \frac{\partial N_1}{\partial x} & \frac{\partial N_1}{\partial y} & 0 & 0 & 0 & 0 & \dots & \frac{\partial N_4}{\partial x} & \frac{\partial N_4}{\partial y} & 0 & 0 & 0 & 0 \end{bmatrix} \tag{7b}$$

$$B_s^{(e)} = \begin{bmatrix} \frac{\partial N_1}{\partial x} & N_1 & 0 & 0 & 0 & 0 & \dots & \frac{\partial N_4}{\partial x} & N_4 & 0 & 0 & 0 & 0 \\ \frac{\partial N_1}{\partial y} & 0 & N_1 & 0 & 0 & 0 & \dots & \frac{\partial N_4}{\partial y} & 0 & N_4 & 0 & 0 & 0 \end{bmatrix}, \tag{7c}$$

where the displacement vector is defined by six DOFs as shown for the first element node as

$$d_1^{eT} = \{u_x, u_y, u_z, \theta_x, \theta_y, \theta_z\}. \tag{8}$$

The element stiffness matrix, defined as the sum of bending membrane and shear, is then obtained by numerical integration for each element by

$$K^e = \int_{\Omega_e} B_b : C_b : B_b d\Omega_e + \int_{\Omega_e} B_m : C_m : B_m d\Omega_e + \int_{\Omega_e} B_s : C_s : B_s d\Omega_e. \tag{9}$$

The vector of nodal forces, which are equivalent to distributed forces P are then calculated as

$$f^e = \int_{\Omega_e} tN \cdot P d\Omega_e + \int_{\Gamma_e} tN \cdot \hat{t} d\Gamma_e, \tag{10}$$

where $\hat{t}$ is the surface traction and Γ_e are the Dirichlet Boundary Conditions (BC). This selective integration for both the stiffness matrix and force vector, using a classical shell theory, is considered the simplest procedure for avoiding shear locking of the element.

Currently the proposed formulation is suitable for the analysis of thin shells of arbitrary shapes. Curved surfaces can be modelled, however in order to capture the curvature with the same accuracy, a greater number of element would be required. More appropriately a curved shell element formulation, with a second order geometric interpolation scheme or higher would be adopted. Where bending and membrane actions do interact and cannot be treated independently [14].

The main purpose of using this custom element is to be able to gather all the information used in the calculation. In the GOEE, values such as the strain-displacement matrices, integration point locations, and other quantities are required. For a typical ABAQUS analysis, this information is either not stored in memory or is not easily available. Ideally, this analysis could be performed using ABAQUS's S4 element if all the information was stored, but due to the black-box nature of the ABAQUS element formulation, this is not possible.

2.2 Primal and Dual Problem Formulation

For the methodology applied to this work, multiple FE evaluations are required. These come from the dual formulation (also called adjunct formulation) for estimating the error [15, 16]. The first evaluation is the standard primal formulation/system. This is a traditional FE evaluation with applied forces resulting in nodal displacements. The systems that are considered in this work are static, so only the stiffness matrix is required for these calculations. More results from the primal solution are required in the GOEE, but are discussed in Section 2.4. For any given system, only one primal solution is required.

The dual formulation is heavily dependent on the selection of the QoI. This evaluates the solution to a generalized force vector to output a QoI via the generalized displacement vector. In general for a static system, this can be expressed as:

$$[K]\{Z\} = \{Q_i\}, \tag{11}$$

where $[K]$ is the stiffness matrix, $\{Z\}$ is the nodal contribution to the QoI, and $\{Q_i\}$ is the generalized forcing vector that depends on the QoI. The stiffness matrix is the same as the primal stiffness in the cases presented in this paper, while the generalized forcing vector is dependent on the type of QoI (average stress, max displacement, etc.) and the location of interest. To calculate $\{Q_i\}$, the QoI must be written as:

$$QoI = \{Q_i\}^T \{u\}, \tag{12}$$

where $\{u\}$ is the displacement field from the primal solution.

In this work, two QoIs are considered: the average stress and average displacement in a region. For the average stress in the y-direction, Eq. 12 is expressed as:

$$\bar{\sigma_y} = \left\{Q_{\sigma_y}\right\}^T \{u\}, \tag{13}$$

where the value of the Q vector is calculated as:

$$\left\{Q_{\sigma_y}\right\} = \frac{1}{\Omega_0} \int_{\Omega_0} C_y : B\,[\hat{e}]\; d\Omega_0, \tag{14}$$

with C_y being the y-component of the material constitutive tensor, B is the deformation matrix (spacial derivatives of the shape functions), $[\hat{e}]$ is a pointer matrix to identify the DOFs associated with the location within the integration, $C : B$ is the double dot product of C and B, and Ω_0 is the domain being considered. This integration is typically decomposed by the the element boundaries since both B and $[\hat{e}]$ are dependent on the which element is being evaluated.

This formulation is useful if a specific region is desired. For this work, point-wise measurements are of interest due to the MARQUESS work-flow. In general, this would require Ω_0 to be very small that causes issue due to the Gauss quadrature integration used in FE. To utilize all the information gathered in the FE analysis, this Q vector is calculated by the approximation of:

$$\left\{Q_{\sigma_y}\right\} \approx \frac{1}{\Omega_0} \sum_{k}^{N_{int}} C_y : B_k\,[\hat{e}]_k\,|J_k| W_k \hat{W}_k, \tag{15}$$

where N_{int} is the number of Gauss quadrature locations in the domain, $|J_k|$ is the determinate of the Jacobian matrix, W_k is the Gauss quadrature weight for the integration point, and $\hat{W}_k$ is a spacial weight distribution to identify importance in the overall calculation. With this formulation, there are two main constraints, written as:

$$\sum_{k}^{N_{int}} |J_k| W_k = \Omega_0 \tag{16a}$$

$$\sum_{k}^{N_{int}} \hat{W}_k = 1. \tag{16b}$$

One reason this approximation is used is due to the fact that all the information about the system is known at the Gauss integration points. The custom made FE stores this information while a typical ABAQUS simulation does not. There are two methods that using spacial weights can help simplify the analysis. The first method is to define a specific region where all the integration points within that domain have a weight value of $\hat{W}_k = 1/N_{int}$. This is the same as defining a specific domain in Eq. 14 where the integral is split along element boundaries. The second method, and the one used in this work, is to apply the weights based on the Euclidean distance from the target location. In this paper, these weights are based on a squared exponential distributed by:

$$\hat{W}_k = a \exp\left(-\frac{|x_k - x_t|^2}{2l^2}\right), \tag{17}$$

where l is a user-defined length, x_t is the location of the center of the distribution, and a is a normalization factor to ensure Eq. 16b is valid.

One caveat of this generation is the multi-physics nature of the shell element formulation. As discussed in Section 2.1, the stiffness is comprised of three separate components (bending, membrane, and shear). Each of these components have individual B and C matrices. In order to calculate the total Q vector, the individual component Q vectors are computed then summed. For example, the bending component of the Q vector is calculated similar to Eq. 15 as:

$$\left\{Q_{\sigma_y}\right\}_b \approx \frac{1}{\Omega_0} \sum_{k}^{N_{int}} C_{b,y} : B_{b,k}\,[\hat{e}]_k\,|J_k| W_k \hat{W}_k, \tag{18}$$

where the subscript b represents the bending component. This calculation is done for each component then summed as:

$$\{Q_{\sigma_y}\} = \{Q_{\sigma_y}\}_b + \{Q_{\sigma_y}\}_m + \{Q_{\sigma_y}\}_s, \quad (19)$$

with the subscripts m and s being the membrane and shear components respectively.

Once the Q vector is determined for a specific QoI, then the FE analysis can be recomputed in order to determine the variable $\{Z\}$, the dual solution. After this computation, then the GOEE can be determined for that particular QoI. In general, there are multiple QoI, thus requiring multiple dual solutions. There is a separate Q vector for each QoI in general, but Section 2.5 discusses a method to approximate some QoI to reduce the total computational time for an analysis.

2.3 Zienkiwicz-Zhu Recovery

ZZ recovery is used in GOEE to create piece wise continuous gradient based fields (for example stress and strain fields)[3, 8]. It is the difference between primal problem solutions and continuous ZZ recovered fields that is treated as an approximation of error in the present work. For the shell element considered, the shape functions are C^0 continuous, such that the derivative (strain) is not continuous across element boundaries. In order to make the strain continuous, the ZZ recovery method is used to create a smooth strain distribution [6, 7]. This section will focus of the ZZ recovery of the strain field due to the utilization in the GOEE, but the ZZ recovery is not restricted to strains.

To perform the ZZ recovery, the strain must be known at specific locations. For the use in FE, these locations are specified as the Gauss integration locations (similar to the calculation of the Q vector in the dual formulation). Once these values are known, then the ZZ recovery can be performed for the location of each node. For each node, the ZZ recovery averages the known strain values at the nearby integration points. In MARQUESS, there are two methods for this averaging. The first method is called the Nearest Neighbour's (NN) approach. This requires the information about the nodal connectivity (which nodes are in each element). The NN approach then takes the nearest integration point location for each element that node is connected to and averages them based on distance. Note that this information is easily available in the mesh data that describes each element as a collection of nodes. An alternative approach is to do a similar weighting that is used in Section 2.2, where the weights are based on the Euclidean distance via a squared exponential such as Eq. 17. One alternative to the formulation in Eq. 17 is to apply user-defined length parameters for each direction. The work presented in this paper uses the NN approach due to the possible complications (especially in the 3D panel) that comes from a distance based ZZ recovery.

Once the nodal values of the recovered strain field are determined, a surface is applied to the system. For an ease-of-use, the element shape functions are used as the basis function for this surface. The equation for this surface is defined as:

$$\epsilon^*(x) = \sum_i N_i(x) [\hat{e}] \{\epsilon^*\}, \quad (20)$$

where $\{\epsilon^*\}$ is the recovered strains at the nodal values, the superscript $*$ representing a recovered value, and $N_i(x)$ are the element shape functions. This function is used in the GOEE for both the primal and dual strains to calculate the estimated error.

2.4 Goal-Oriented Error Estimator

The main purpose of this work is to create an error estimator that has physical significance to aid design engineers in the design and analysis of an aerospace system. To create this error estimator, two main methods are used: ZZ recovery and dual problems. Both of these are discussed in Section 2.3 and Section 2.2 respectively.

This formulation of the GOEE closely follows the work in [5] with slight differences on how the dual problem is performed. The calculation is based on the energy norm, which is defined as:

$$|H|_e = \int_\Omega H : C : H d\Omega, \quad (21)$$

where H is any quantity of interest, $|H|_e$ is the energy norm of H, C is the material constitutive tensor, and Ω is the domain of interest. In a typical system, one GOEE that can be used is the energy norm of the difference between the ZZ recovered QoI and the FE values [8]. However, this does not account for the dual formulation used in this work.

To account for the dual problem formulation used in this analysis, the GOEE is defined as:

$$GOEE = \int_\Omega (\epsilon_u^* - \Delta u_h) : C : (\epsilon_z^* - \Delta z_h) d\Omega, \quad (22)$$

with ϵ_u^* and ϵ_z^* being the ZZ recovered strain for the primal and dual problem respectively, u_h is the displacement determined by the primal FE problem, z_h is the generalized displacement from the dual FE problem (in units of the force normalized QoI), and Δ is a collection of spacial derivatives. In simplified terms, the difference $(\epsilon^* - \Delta u_h)$ is equivalent to the difference of applying the shape function interpolation before and after the differentiation. For a refined mesh, this difference is nearly zero while a difference will occur for a course mesh.

Similar to the method used to calculate the Q vector in Section 2.2, the GOEE is comprised of three components (bending, membrane, and shear). For the bending component, Eq. 22 is calculated as:

$$GOEE_b = \int_\Omega (\epsilon^*_{u,b} - \Delta u_{h,b}) : C_b : (\epsilon^*_{z,b} - \Delta z_{h,b}) d\Omega. \tag{23}$$

This is then performed for each component then summed as:

$$GOEE = GOEE_b + GOEE_m + GOEE_s. \tag{24}$$

In the general case, the GOEE is calculated for each QoI. This value can be stored as a scalar for the total error, or as an array to signify specific region's (or element's) contribution to the error. Storing this information for each element is one method to identify "hotspots" where the design engineer can focus attention to for mesh refinement or design modifications.

2.5 Bayesian Recovery of the Error Field

While the calculation of the GOEE can be done for each QoI, this can take a lot of computational time. It effectively runs a full FE model for each QoI and is difficult for large systems such as aircraft. One method used to reduce this computational burden is through the use of GP or Bayesian response surface identification.

The basis of the Bayesian response surface is to use a select number of evaluations (called training points) in order to get a stochastic response surface that can be easily sampled at selected locations (called test points) [17]. This surface is made predominately through a kernel (or covariance) function. There are many choices for the kernel function (many described in [17]) that can better characterize the response depending on the analysis being performed. For this work, a Squared Exponential (SE) kernel is used that is expressed as:

$$k(x, x') = exp\left(\frac{-|x - x'|^2}{2l^2}\right), \tag{25}$$

with x and x' being two locations and l is a length hyper-parameter. One aspect of this kernel function is that it is only dependent on the distance between the two locations (stationary). Future work for this project is the inclusion of the Matérn kernel since it better represents the physics of a FE analysis and is expected to provide a more accurate surface [17]. One special effect of using this is:

$$k(f(x), f(x')) = k(x, x') = exp\left(\frac{-|x - x'|^2}{2l^2}\right). \tag{26}$$

This allows for the covariance of the response to be described by the covariance of the evaluation locations [17].

The first step in defining a Bayesian surface is the evaluation of the training points to create the known response space. For this work, these are done with a FE analysis while this is also possible with experimental measures. These training points give observations as:

$$Y = f(X) + \epsilon, \tag{27}$$

where Y is the training point observations at locations X, $f(x)$ is the simulation function (in this case the FE analysis), and ϵ is Gaussian noise with variance σ_n^2. This leads the covariance between the training point evaluations to be described as:

$$cov(Y) = K(X, X) + \sigma_n^2 I, \tag{28}$$

where K is a matrix such that $K_{i,j} = k(x_i, x_j)$ and I is an identity matrix. This formulation is useful if scalar values are known at exact locations, such as experimental measurements. Although other approaches are possible, this work uses the simplified expression that the dual results are scalar values known at the evaluated locations.

In this work, for simplicity, the test points are taken as each nodal location of the system, and the training points are either manually selected by the user or selected as random nodal locations. For either case of the training points, a total response location vector X_* is computed as the concatenation of the training and test locations. Because of this concatenation, a training point identification matrix can be defined as:

$$H = [I, 0], \tag{29}$$

where I is an identity matrix with a size of the number of training points (N_{train}) and 0 being a matrix of zeros of size $N_{train} \times N_{test}$. With the known observations, a joint normal distribution can be described as:

$$\begin{bmatrix} \mathrm{Y} \\ f_* \end{bmatrix} \sim \mathcal{N}\left(\mathbf{0}, \begin{bmatrix} H\Sigma H^T + \sigma_n^2 I & H\Sigma \\ \Sigma H^T & \Sigma \end{bmatrix}\right), \tag{30}$$

where f_* is the test location responses and $\Sigma_{i,j} = k(x_i, x_j)$ is the covariance of the locations (also known as the prior distribution) for all the locations in X_*. Knowing this joint distribution, a predictive distribution can be determined for f_* ([17] for more specific details). This results in the mean ($\bar{f}_*$) and covariance of f_* being calculated as:

$$\bar{f}_* = \Sigma H^T (H\Sigma H^T + \sigma_n I)^{-1} Y \tag{31a}$$

$$cov(f_*) = \Sigma - \Sigma H^T (H\Sigma H^T + \sigma_n I)^{-1} H\Sigma. \tag{31b}$$

This predicted joint normal distribution can be sampled to get the predicted distribution for each nodal location.

For the use in this paper, the Bayesian surface is used to describe the GOEE field of the 3D system. This is used to reduce the computational time since only a few full FE simulations are performed while the other locations are sampled from a simple distribution. Selection of these few FE simulations are based on a random selection of nodes. However, there is one required simulation that is enforced. This is a dual problem based at the applied force location. In addition to the selected FE simulations, the Boundary Condition (BC) nodes are also enforced as training locations. For this work, it is assumed that the point-wise GOEE is zero at the BC to enforce the Dirichlet BC.

3 2D Flat Panel

3.1 System Description

In order to demonstrate the general work-flow of this analysis (minus the GP), a 2D flat panel is used for verification. This panel uses the full shell element formulation previously described in Section 2.1. The loading condition for this system is a quadratic tensile loading such that the edges have zero force applied to them. This can be seen in Fig. 2 in addition to the BC of a pinned bottom surface. The maximum applied force (at the center) is based on the maximum pressure loading of 100 KN/m resulting in 1 KN force for the nominal mesh. This was chosen to obtain a stress at the center of the system to be near 100 MPa.

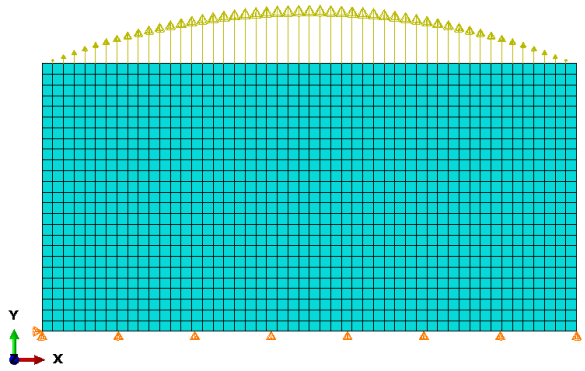

Figure 2: Mesh, loading and BC of 2D system

The material properties of this system are based on 2024 aluminium and reasonable physical parameters. These properties are the same for the 2D and 3D systems tested in this work. For the 2024 aluminium: the Young's modulus is assumed to be 73.1 GPa, and the Poisson's ratio is 0.33. The thickness of the shell elements are all assumed to be 1 mm thick.

For the simplified 2D panel, only one QoI is selected. This is the stress at the center of the panel, which is calculated using a weighting function of a squared exponential for $\hat{W}_k$ in Eq. 15. For this QoI, the user-defined length is set to the length of 10 mm. This is thought of as the spacial standard deviation in all directions. The determination of this length (by expert opinion or maximum likelihood method) will but further explored in future work.

For this system, three meshes are analysed to show the convergent nature of the GOEE. The nominal mesh is defined with an element edge-length of 10 mm, resulting in a grid of 50×25 elements. In order to test the convergent nature of the GOEE (more refined mesh should have smaller GOEE), the other two meshes are defined as half and double the element edge-length.

3.2 Results

Since the 2D panel only has one QoI, this results section will focus on the main steps while the 3D system will focus on the Bayesian analysis. For this work, the FE simulation is only performed for the primal solution while the dual solutions are solved within Python using the stiffness matrix that is outputted by the FE analysis via Eq. 11. In the current implementation, the FE simulation produces text files that in read into Python and used in this analysis. Currently, the simulation creates 10 files that are imported into Python, including:

- The stiffness matrix. This is written on an element-by-element basis in lower triangular format.
- The displacement for each DOF at each node.
- The nodal locations in the global coordinate system.
- The nodal definition for each element. Contains the information about what nodes are in each element.
- The rotation matrix for each element. This is only used in the 3D system.
- The Gauss integration point locations in the global coordinate system.
- The individual membrane, bending, and shear B matrices at each integration location.
- The determinant of the Jacobian matrix at each integration point.

With this information, the stress and strains are calculated at each Gauss integration location. The strains are stored to be used for Δu_h and the stresses are used for verification. Using these integration values, the ZZ recovery is performed for each node then stored in ϵ_u^*. After the primal solution is calculated, the Q vector is

calculated. Using the primal stiffness matrix and this Q vector, the dual displacement Z vector is calculated. With the Z nodal vector, the dual strains are calculated at each integration location and stored as Δz_h. With these values, the ZZ recovery is also performed for the dual strains to be stored in ϵ_z^*. With these pieces of information, the GOEE is calculated for the QoI by separating the domain into the elements and using Gauss quadrature to evaluate the integral.

For this system, three different meshes are tested. The results for all these simulations are summarized in Tab. 1. In general, the GOEE follows the expected pattern of decreased error with a more refined mesh. The results in Tab. 1 are based on a QoI of approximately 91.7 MPa. The largest error was 0.31 MPa, which is less than 1% error. This small error is partially due to the selected QoI and the simple nature of the system.

Table 1: Total GOEE Results

Description	GOEE
Half Mesh	310 KPa
Nominal Mesh	75 KPa
Double Mesh	19 KPa

While the percent error is small, one of the main purposes of this analysis is to highlight the areas of highest error. For the nominal mesh, the hot-spots are shown in Fig. 3. This shows that the elements near the center (where the stress is being evaluated) have the largest error. For ease of viewing, the contour plot shown in Fig. 3 is the magnitude of the total GOEE for each element. Some of these elements contribute to higher estimated stress while others contribute to lower stress. This plot is also generated for the other meshes, but not shown here. These identify the same hot-spot areas of high importance with different scaling.

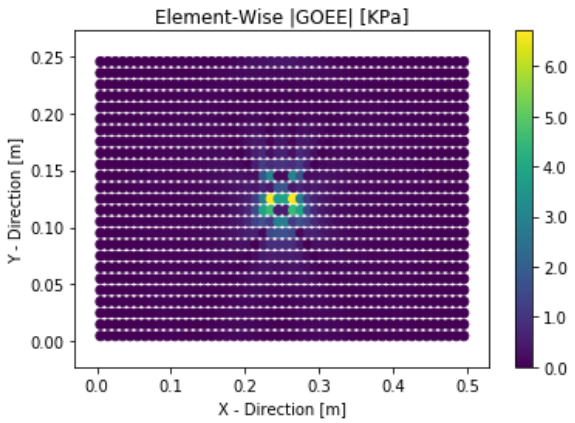

Figure 3: Element based GOEE to identify hot-spot locations

One important aspect of Fig. 3 is that the GOEE is symmetric around $x = 0.25$. This is due primarily due to the symmetric loading and the QoI being at the center. The hot-spot identification near the center meets the expected result of locations near the point of interest. Overall, this example shows the GOEE workflow without the GP sampling.

4 Stiffened 3D Panel

4.1 System

The second example is a representative 3D stiffened panel, formed of a flange and longitudinal stiffener (web). The structural component is used to represent a simplified flat section of a typical T-stringer stiffened panel, which would form part of a larger representative aircraft wing or fuselage structure. The idealised T-sectional component, has a length of 0.5m by 0.2m wide and a web height of 0.05m. Both the flange and web thicknesses are 1 mm.

The finite element model, shown in Fig. 4, is formed from the same shell element, with identical material properties as for the 2D system described in Section 3 and a nominal mesh size of 10 mm. The boundary conditions and loading are similar to a simple cantilever beam, with the cross-section at one end being pinned supported at all nodes with a point loading applied as a 1.5KN force at the intersection between the flange and web on the opposite free end.

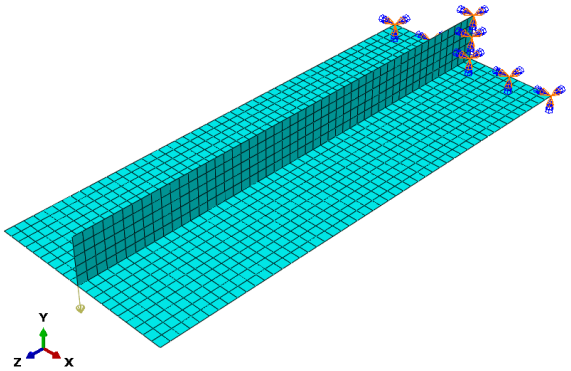

Figure 4: 3D system shell element model showing mesh, boundary conditions and applied load

The loading and material properties where chosen to ensure the beam remains elastic with the applied load. The maximum end deflection of the beam is within 1% compared against the analytical solution and ABAQUS's S4 element for compared displacements and stresses. Shell element results for the scaled deformation and averaged von Mises stress are shown in Fig. 5.

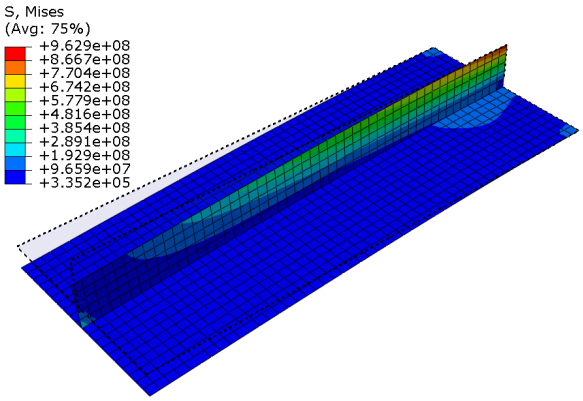

Figure 5: Von Mises stress, with the deformation (scale factor of 1) compared against the undeformed state

Using this implementation, models can be either manually generated or imported from ABAQUS (shown in Fig. 4) into the custom finite element code. For visualisation the returned results are imported into ABAQUS CAE's Viewer module. Python scripting is used to generate an ODB file, building the mesh geometry and creating history output data by importing the external result files for displacements, stresses and GOEE.

4.2 Results

The first result for the stiffened 3D panel is the case where a dual problem was performed for each node. For a more realistic system, this would not be feasible, but can be taken as the reference GOEE field that the Bayesian prediction is compared to. To illustrate this field, a color plot is mapped onto the geometry and is shown in Fig. 6. For the dual problem formulations, the characteristic length used is the edge length of an element (10 mm).

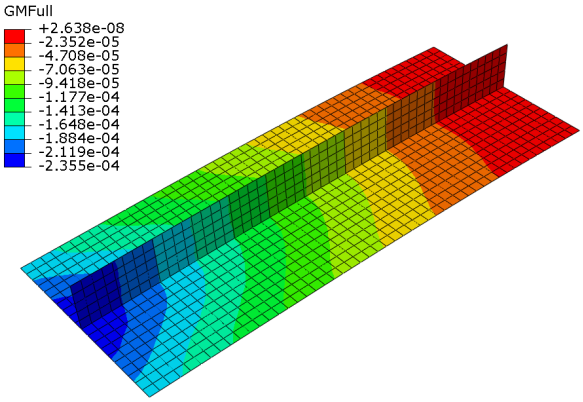

Figure 6: Reference GOEE field to identify hot-spot locations

The main aspect of Fig. 6 is that error of the z-direction displacement is largest at the applied force location, which also has the largest displacement. This follows the design common-sense that a refined mesh near the loading will increase the accuracy. In total, there are $1,300$ FE simulations used for Fig. 6 and takes about two hours to perform all the simulations, keeping in mind that this system is small compared to the intended systems. For realistic systems with hundreds of thousands of nodes, performing this many simulations is not practical. In order to reduce the computational burden, the GOEE is predicted with a GP using only a subset of 100 FE simulations.

The reduced basis for the GP uses the results from 100 dual solutions. For these dual problems, the center is selected as random nodes. This is thought of as a preliminary investigation without an investigation into optimal selection of locations. For the GP kernel, a characteristic length was selected to be four elements (40 mm). This is selected to give a disperse representation for the GP. Future work includes the selection of this length via maximum likelihood opposed to the manual selection currently used. The predictive mean of the GOEE field is presented in Fig. 7.

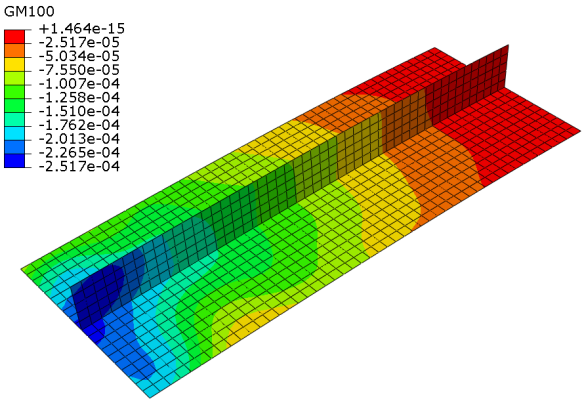

Figure 7: 100 Dual solution recovered GOEE field

For the majority of this recovered field, there is little differences between the true and recovered fields. However, in particular, there are two main locations where there is a difference. The first location is the corner of the web portion. In the true field, there is little difference between the corner and the applied force location, while the recovered field has a larger difference. This is specific to the selected 100 dual problems. By placing a dual solution centered near that corner, the difference between the true and recovered fields decreases. The second location of a noticeable difference is near the bottom edge. This is noticed by the yellow contour surrounded by green. Despite these two locations, the recovered GOEE field matches well. One note on these results is that there is no assumption of symmetry along the web section made in this system. If this assumption is made, then the 100 simulations would

only be required to span half the space, thus producing an expected more accurate mean GOEE field.

5 Conclusions and Remarks

This work demonstrates the use of Bayesian regression of a goal oriented error estimator field in 3D shell element structures. The work in this paper is intended to be used by design engineers in the design of large aerospace systems. This includes the combination of several techniques, primarily Zienkiwicz-Zhu recovery and dual problem formulation for GOEE evaluation.

This methodology is applied to two separate systems, one 2D system looking at the mean stress at the center and one 3D system investigating the average displacement while investigating the computational reduction of using the Gaussian process to reconstruct the error field. The reconstruction using less than 10% of the simulations produces an accurate field with a minor difference at two noticeable locations of difference. This difference and locations can be adjusted based on the locations of the dual problems. Future work in this methodology is to determine error bounds for a specified number of dual problems.

In addition to the determination of error bounds, future work is focused on the industrial size implementation. For this work, a custom finite element solver is used and outputs the stiffness matrix and the results from the primal solution, and the dual problems use this outputted stiffness matrix to create the dual solutions. The main aspect for the future work is to use ABAQUS to perform both the primal and dual problems. This will be done by developing a USER-ELEMENT (UEL) that implements the shell formulation used in this work. Once the implementation into ABAQUS is complete, future work is to include the bottom-up aspect of MARQUESS.

Acknowledgements

This project is funded by the Clean Sky 2 Joint Undertaking under the European Union's Horizon 2020 research and innovation programme under grant agreement No 754581.

References

[1] X. Zou, S. Yan, M. Matveev, J. P. Rouse, I. A. Jones, M. Hamadi, and M. Fouinneteau. Comparison of interface modelling strategies for predicting delamination in composite l-angle sections under four-point bending. composite structures. *Journal of Composite Structures*, 2019. Submitted.

[2] X. Zou, S. Yan, J. Rouse, M. Matveev, S. Li, I. A. Jones, M. Hamadi, and M. Fouinneteau. The identification of failure initiation hotspots in idealised composite material component models using a "bottom-up database" method. *Proceedings of the 18th European Conference on Composite Materials*, 2018.

[3] Thomas Grätsch and Klaus-Jürgen Bathe. A posteriori error estimation techniques in practical finite element analysis. *Computers & structures*, 83(4-5):235–265, 2005.

[4] Karan S Surana, Aaron D Joy, and JN Reddy. Error estimations, error computations, and convergence rates in fem for bvps. *Applied Mathematics*, 7(12):1359–1407, 2016.

[5] Octavio Andres González-Estrada, E Nadal, JJ Ródenas, Pierre Kerfriden, Stéphane Pierre-Alain Bordas, and FJ Fuenmayor. Mesh adaptivity driven by goal-oriented locally equilibrated superconvergent patch recovery. *Computational Mechanics*, 53(5):957–976, 2014.

[6] JZ Zhu and OC Zienkiewicz. Adaptive techniques in the finite element method. *Communications in applied numerical methods*, 4(2):197–204, 1988.

[7] Olgierd C Zienkiewicz and Jian Z Zhu. A simple error estimator and adaptive procedure for practical engineerng analysis. *International journal for numerical methods in engineering*, 24(2):337–357, 1987.

[8] M Ainsworth, JZ Zhu, AW Craig, and OC Zienkiewicz. Analysis of the zienkiewicz–zhu a-posteriori error estimator in the finite element method. *International Journal for numerical methods in engineering*, 28(9):2161–2174, 1989.

[9] ABAQUS Dassault Systemes Simulia Corporation. Documentation, 2019.

[10] Junuthula Narasimha Reddy. Mechanics of laminated composite plates and shells: theory and analysis, 2003.

[11] Yan Shang, Song Cen, and Chen-Feng Li. A 4-node quadrilateral flat shell element formulated by the shape-free hdf plate and hsf membrane elements. *Engineering Computations*, 33(3):713–741, 2016.

[12] Young W Kwon and Hyochoong Bang. The finite element method using matlab, 2018.

[13] Eduardo N Dvorkin and Klaus-Jürgen Bathe. A continuum mechanics based four-node shell element for general non-linear analysis. *Engineering computations*, 1(1):77–88, 1984.

[14] R. L. Taylor O. C. Zienkiewicz. The finite element method. fifth edition. *Bautechnik*, 79(2):122–123, 2002.

[15] KG Van der Zee and CV Verhoosel. Isogeometric analysis-based goal-oriented error estimation for free-boundary problems. *Finite Elements in Analysis and Design*, 47(6):600–609, 2011.

[16] Fredrik Larsson, Peter Hansbo, and Kenneth Runesson. Strategies for computing goal-oriented a posteriori error measures in non-linear elasticity. *International Journal for Numerical Methods in Engineering*, 55(8):879–894, 2002.

[17] C. E. Rasmussen and C. K. I. Williams. *Gaussian Processes for Machine Learning*. The MIT Press, 2006. www.GaussianProcess.org/gpml.